PRAMANA
— journal of
physics

Vol. 69, No. 6
December 2007
pp. 981–987

A beam test of prototype time projection chamber using micro-pattern gas detectors at KEK

MAKOTO KOBAYASHI, on behalf of part of the ILC–TPC Collaboration
High Energy Accelerator Organization (KEK), Tsukuba 305-0801, Japan
E-mail: makoto.kobayashi.exp@kek.jp

Abstract. We conducted a series of beam tests of prototype TPCs for the international linear collider (ILC) experiment, equipped with an MWPC, a MicroMEGAS, or GEMs as a readout device. The prototype operated successfully in a test beam at KEK under an axial magnetic field of up to 1 T. The analysis of data is now in progress and some of the preliminary results obtained with GEMs and MicroMEGAS are presented along with our interpretation. Also given is the extrapolation of the obtained spatial resolution to that of a large TPC expected as the central tracker of the ILC experiment.

Keywords. Time projection chamber; micro-pattern gas detectors; micro-mesh gaseous structure; gas electron multiplier; international linear collider; spatial resolution.

PACS Nos 29.40.Cs; 29.40.Gx

1. Introduction

One of the major physics goals of the future linear collider experiment is to study properties of the Higgs boson, which is expected to be well within the reach of the center-of-mass energy of the machine [1,2]. This goal demands unprecedented high performance of each detector component. For example, the central tracker is required to have good spatial resolution, high two-track resolving power, and high momentum resolution, for precise reconstruction of hard muons and each of the charged particle tracks in dense jets.

A time projection chamber (TPC) is a strong candidate for the central tracker of the experiment since it can cover a large volume with a small material budget while maintaining a high tracking density (granularity). If micro-pattern gas detectors (MPGDs) micro-mesh gaseous structure (MicroMEGAS) [3], gas electron multiplier (GEM) [4] etc.) are employed as the detection devices of the TPC, instead of the conventional multi-wire proportional chambers (MWPCs), one can expect better spatial resolution at a lower gas gain and higher granularity, with a smaller or negligible $E \times B$ effect at the entrance to the detection plane. Furthermore, the MPGDs have inherently smaller positive-ion back flow rates than MWPCs. We

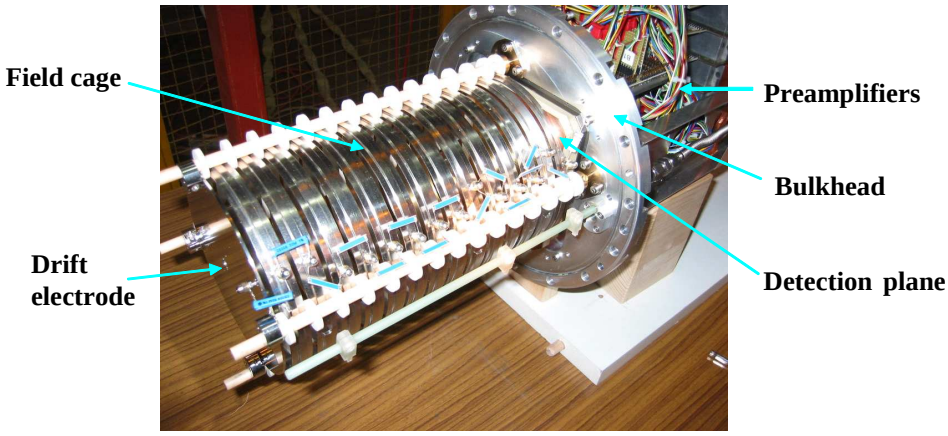

Figure 1. Photograph of the prototype just before installation into the gas vessel.

therefore constructed a small prototype TPC with a replaceable readout device (MWPC, MicroMEGAS or triple GEM) and have conducted a series of beam tests at KEK in order to study the performance, especially its spatial resolution under an axial magnetic field.

We begin with brief descriptions of the prototype TPC and the experimental set-up. Next, some preliminary results are presented along with our interpretation, in which special emphasis is placed on an analytic expression of the spatial resolution. Finally, the spatial resolution of the ILC–TPC is estimated from that measured with the prototype.

2. Experimental set-up

A photograph of the prototype is shown in figure 1. It consists of a field cage and an easily replaceable gas amplification device attached to one end of the field cage. Gas amplified electrons are detected by a pad plane at ground potential placed right behind the amplification device. A drift electrode is attached to the other end of the field cage. The maximum drift length is about 260 mm.

The pad plane, with an effective area of $\sim 75 \times 75$ mm^2, has 12 pad rows at a pitch of 6.3 mm, each consisting of 2×6 (1.27×6) mm^2 rectangular pads arranged at a pitch of 2.3 (1.27) mm when combined with MicroMEGAS (GEMs). Pad signals are fed to charge sensitive preamplifiers located on the outer surface of the bulkhead of the gas vessel behind the pad plane. The amplified signals are sent to shaper amplifiers with a shaping time of 500 ns in the counting room via twisted-pair cables, and then processed by 12.5 MHz digitizers.

The mesh of MicroMEGAS, made of 5-μm thick copper, has 35 μm holes spaced at intervals of 61 μm. The distance between the mesh and the pad plane is maintained at 50 μm by kapton pillars arranged in between. The typical gain is about 3650 at the mesh potential of -320 V. The triple GEM, CERN standard, has two 1.5 mm transfer gaps and a 1 mm induction gap. The transfer and induction fields are

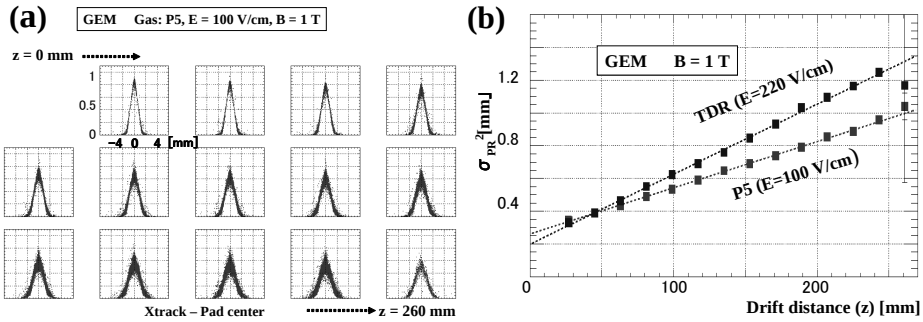

Figure 2. (**a**) Pad responses for different drift distances. (**b**) Pad response width squared ($\sigma^2_{\rm PR}$) vs. drift distance (z). The width of pad response is parametrized as $\sigma^2_{\rm PR} = \sigma^2_{\rm PR0} + D^2 \cdot z$, with D being the diffusion constant.

about 2 kV/cm and 3 kV/cm, respectively. The typical total effective gain in a P5 (TDR) gas is about 3000 with 335 (340) V applied across each GEM foil.

The chamber gases are Ar–isobutane (5%) for MicroMEGAS, and a TDR gas (Ar–methane (5%)–carbon dioxide (2%)) or a P5 gas (Ar–methane (5%)) for GEMs, at atmospheric pressure and room temperature. The gas pressure and the ambient temperature are continuously monitored since they are not controlled actively. The drift-field strengths are 220, 235 and 100 V/cm, respectively for Ar–isobutane, TDR gas and Ar–methane.

The prototype TPC is placed in the uniform field region of a superconducting solenoid without return yoke, having a bore diameter of 850 mm, effective length of 1000 mm, and the maximum field strength of 1.2 T. The prototype was then subjected to the beam, mostly 4 GeV/c pions, at the $\pi 2$ test beam facility of the KEK proton synchrotron.

3. Preliminary results

In this section we show some preliminary results of the analysis up to now, only for the data taken with an axial magnetic field [4a] of 1 T and with tracks perpendicular to the pad rows, because of the limited space available. The results of analytic evaluations are used or presented here without comments. Readers are therefore advised to read the full paper with an appendix [5], and/or to take a look at the slides available on-line [6], where the analytic method is briefly summarized and illustrated.

The observed pad responses for different drift distances (z) are shown in figure 2a while the widths of distributions are plotted as a function of the drift distance in figure 2b. Figures 3a and 3b show the spatial resolution in the pad row direction, obtained with a charge centroid method, plotted against the drift distance (z), respectively for the MicroMEGAS and triple GEM readout, along with the results of the analytic calculations. In the calculation the pad response function (PRF) was assumed to be a δ function for the MicroMEGAS and a Gaussian for the GEMS [6a].

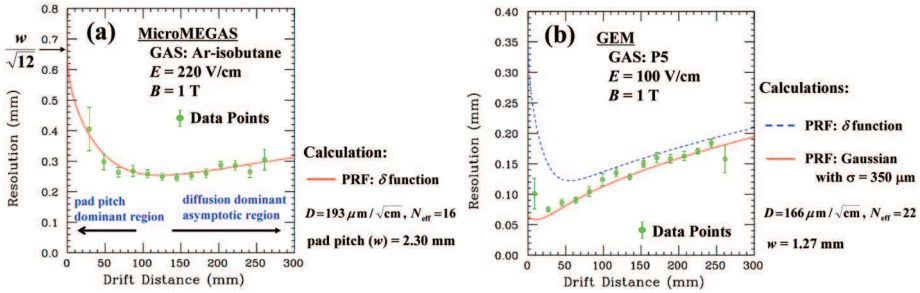

Figure 3. (**a**) Spatial resolution vs. z obtained with MicroMEGAS, $w = 2.3$ mm, gas: Ar–isobutane (5%). (**b**) Spatial resolution vs. z obtained with GEMs, $w = 1.27$ mm, gas: Ar–methane (5%).

Table 1. Asymptotic behavior at long drift distances under $B = 1$ T.

Detection device Gas	MicroMEGAS Ar–isobutane (5%)	GEM TDR	GEM Ar–methane (5%)
(a) Pad response			
σ_{PR0} (μm)	758 ± 91	432 ± 3	511 ± 2
$w/\sqrt{12}$ (μm)	664	367	
D ($\mu\mathrm{m}/\sqrt{\mathrm{cm}}$)	194 ± 18	213 ± 1	168 ± 1
D (MAGBOLTZ)	193	209	166
(b) Spatial resolution			
σ_{X0} (μm)	161 ± 54	44 ± 10	42 ± 17
$w/\sqrt{12 \cdot N_{\mathrm{eff}}}$ (μm)	166 ± 42	86 ± 3	78 ± 4
$D/\sqrt{N_{\mathrm{eff}}}$ ($\mu\mathrm{m}/\sqrt{\mathrm{cm}}$)	48 ± 12	47 ± 1	35 ± 2
N_{eff}	16 ± 8	20 ± 1	22 ± 2

The obtained behavior of the pad response, and the spatial resolution at long drift distances [6b] are compared with expectations in table 1. The comparisons show

1. σ_{PR0} is in reasonable agreement with the expectation ($\sqrt{w^2/12 + \sigma^2_{\mathrm{PRF}}}$) if the contribution of σ_{PRF} is taken into account (in the case of GEMs).
2. σ_{X0} is in good agreement with the expectation ($w/\sqrt{12 \cdot N_{\mathrm{eff}}}$) for the MicroMEGAS, and better than this for the GEMs because of the significant charge spread in the transfer and induction gaps.
3. The values of diffusion constant (D) are comparable to those given by the simulation (MAGBOLTZ [7]).
4. N_{eff} (16–22) is significantly smaller than the average number of drift electrons per pad row (∼71) [8].

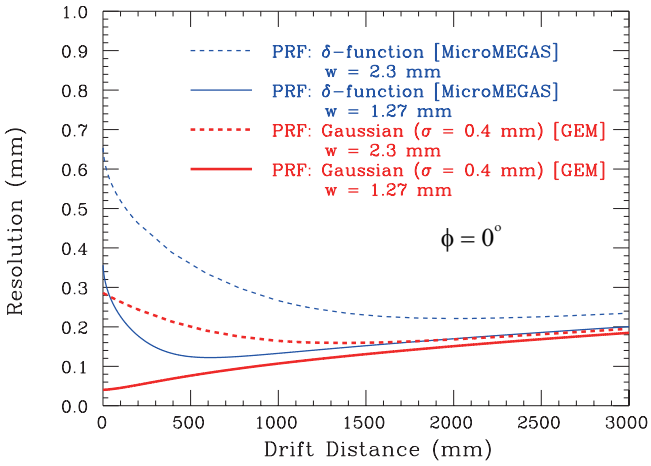

Figure 4. Expected spatial resolutions of the ILC-TPC obtained with MicroMEGAS or GEMs. Gas: Ar–methane (5%), $E = 100$ V/cm, $B = 4$ T ($D = 50\ \mu\text{m}/\sqrt{\text{cm}}$), and $N_{\text{eff}} = 22$.

4. Expected spatial resolution of the ILC–TPC

The calculated spatial resolutions of the ILC–TPC at $B = 4$ T are shown in figure 4 for tracks perpendicular to the pad row. In the calculations the values of diffusion constants (D) given by MAGBOLTZ were used. The figure tells us that under a strong magnetic field it is important to reduce the pad-pitch dominant region (at small drift distances) in the ILC–TPC by enhancing the charge sharing among the readout pads, in order to maintain a good resolution over the entire sensitive volume.

There are several possibilities to realize effective charge sharing:

- Zigzag (chevron) pads.
- A smaller pad pitch with a larger number of readout channels.
- Defocussing of electrons after gas amplification (natural dispersion in the transfer and induction gaps of GEMs, *stochastic* PRF).
- Use of resistive anode technique with a moderate number of readout channels (applicable to both GEMs and MicroMEGAS, *static* PRF) [9].
- Pixel readout (Digital TPC) [10].

5. Summary

To summarize, the prototype TPC equipped with a MicroMEGAS or GEMs operated stably during the beam tests. The tests provided us with an insight into the spatial resolution along the pad row direction, which is achievable with a TPC equipped with an MPGD readout.

- The obtained spatial resolution is understood in terms of pad pitch, diffusion constant, PRF, and the effective number of electrons.
- The expected resolution can be estimated by a numerical calculation (NOT a Monte-Carlo) for given geometry, gas mixture and PRF if the relevant parameters are known.
- The calculation is based on a simple formula, easy to code and fast, though it is applicable only to tracks perpendicular to the pad row.
- In the case of MicroMEGAS, the spatial resolution as a function of the drift distance is well described by the analytic formula, assuming δ function for PRF.
- In the case of GEMs, the spatial resolution as a function of the drift distance is satisfactorily described by the analytic formula, assuming a Gaussian for PRF with the width determined from the intercept of the pad-response width squared as a function of the drift distance.
- It is important to make the pad pitch small, *physically or effectively*, in order to reduce both the overall offset term (σ_{X0}) at long drift distances and the resolution degradation due to finite pad pitch at short drift distances.
- The spatial resolution required for the ILC–TPC (100–200 μm for the maximum drift distance of $\sim$2.5 m) is now within reach for tracks perpendicular to the pad row.

Acknowledgements

The author would like to thank the people at Indian Institute of Science for their support and hospitality. He is also grateful to many colleagues in the ILC–TPC collaboration for their continuous encouragement and support, and to the people at KEK Cryogenics Science Center and the members of IPNS cryogenic group for the preparation and the operation of the superconducting magnet.

References

[1] TESLA Technical Design Report, DESY 2001-011.
[2] GLC Project Report, KEK Report 2003-7.
[3] Y Giomataris *et al*, *Nucl. Instrum. Methods* **A376**, 29 (1996)
[4] F Sauli, *Nucl. Instrum. Methods* **A386**, 531 (1997)
[4a] It should be pointed out here that the pad rows were *effectively* staggered even in the case of the MicroMEGAS readout since the beam had a small but finite average angle of $\sim 3^\circ$ with respect to the pad-row normal
[5] M Kobayashi *et al*, KEK Preprint 2006-35
[6] http://www.tifr.res.in/~ lcws06/
[6a] PRF is the avalanche charge spread on the pad plane for a *single* drift electron and should not be confused with the pad response. In the case of MicroMEGAS it is much smaller than the pad pitch (2.3 mm) and is, therefore, neglected. The width (standard deviation) of the Gaussian PRF for the triple GEM has been determined from the intercept of the pad-response width squared vs. z (figure 2b): $\sigma^2_{\rm PR} = \sigma^2_{\rm PR0} + D^2 \cdot z$

with $\sigma^2_{\rm PR0} = w^2/12 + \sigma^2_{\rm PRF}$ [5], where the pad pitch $w = 1.27$ mm and $\sigma_{\rm PRF} \sim 511$ μm, yielding $\sim$356 μm for $\sigma_{\rm PRF}$. The value of $\sigma_{\rm PRF}$ thus obtained is consistent with a simple estimation taking into account only the diffusion in the transfer and induction gaps

[6b] When PRF is δ function the asymptotic behavior of the spatial resolution at long distances (diffusion dominant asymptotic region) is described by $\sigma^2_X \equiv \sigma^2_{X0} + D^2_X \cdot z \sim 1/N_{\rm eff} \cdot (w^2/12 + D^2 \cdot z)$, where $N_{\rm eff}$ is the effective number of electrons and D is the diffusion constant [5]

[7] S F Biagi, *Nucl. Instrum. Methods* **A421**, 234 (1999)

[8] M Kobayashi, *Nucl. Instrum. Methods* **A562**, 136 (2006)

[9] M S Dixit *et al*, *Nucl. Instrum. Methods* **A518**, 721 (2004)

[10] P Colas *et al*, *Nucl. Instrum. Methods* **A535**, 506 (2004)